Foldamers

International Edition: DOI: 10.1002/anie.201902378
German Edition: DOI: 10.1002/ange.201902378

Light-Controlled Conformational Switch of an Aromatic Oligoamide Foldamer

Bappaditya Gole, Brice Kauffmann, Victor Maurizot, Ivan Huc, and Yann Ferrand**

Abstract: *An aromatic oligoamide sequence composed of a light-responsive diazaanthracene-based aromatic β-sheet flanked by two variable diameter helical segments was prepared. Structural investigations revealed that such oligomers adopt two distinct conformations: a canonical symmetrical conformation with the two helices stacked above and below the sheet, and an unanticipated unsymmetrical conformation in which one helix has flipped to directly stack with the first helix. Photoirradiation of the foldamer led to the quantitative, and thermally reversible, formation of a single photoproduct resulting from the [4+4] cycloaddition of two diazaanthracenes within the aromatic β-sheet. NMR and crystallographic studies revealed a parallel arrangement of the diazaanthracene photoproduct and a complete conversion into a symmetrical conformation requiring a rearrangement of all unsymmetrical conformers. These results highlight the potential of foldamers, with structures more complex than isolated helices, for the design of photoswitches showing nontrivial nanometer scale shape changes.*

Molecular folding constitutes a formidable tool to implement switching, controlled motion, and response to external stimuli at the nanometer scale. As best exemplified by the folded conformations of proteins, complex arrays of intramolecular interactions and a hierarchical structure composed of several sheet, turn, loop, and helix subunits, may give rise to sophisticated allosteric behavior.[1] It may also allow for signal transduction across, for example, bilayer membranes through subtle conformational changes mediated by either guest binding or by a simple phosphorylation, as in G-protein coupled receptors,[2] or large-scale controlled molecular motions coupled to the consumption of chemical energy as performed by kinesin[3] or myosin.[4]

[*] Dr. B. Gole, Dr. V. Maurizot, Dr. Y. Ferrand
CBMN (UMR5248), Univ. Bordeaux – CNRS – IPB
Institut Européen de Chimie et Biologie
2 rue Escarpit, 33600 Pessac (France)
E-mail: y.ferrand@iecb.u-bordeaux.fr
Dr. B. Kauffmann
Université de Bordeaux, CNRS, INSERM, UMS3033
Institut Européen de Chimie et Biologie (IECB)
2 rue Robert Escarpit, 33600 Pessac (France)
Prof. I. Huc
Department of Pharmacy and Center for Integrated Protein Science,
Ludwig-Maximilians-Universität
Butenandtstr. 5–13, 81377 München (Germany)
E-mail: ivan.huc@cup.lmu.de
Supporting information and the ORCID identification number(s) for the author(s) of this article can be found under: https://doi.org/10.1002/anie.201902378.

Likewise, synthetic foldamers[5] show promise in the design and fabrication of artificial systems endowed with comparable properties and constitute an underexplored approach to artificial molecular switches and motors.[6,7] Until now, most investigations have concerned isolated helically folded oligomers or polymers. Helices may undergo handedness reversal upon interacting with chiral guests, thus leading to chiral amplification and, eventually, kinetic trapping of chiral helical states,[8] or to the transfer of chiral information from one end of the helix to the other.[9] They may also undergo equilibria between folded and unfolded states triggered by light,[10] springlike extensions and contractions mediated by metal-ion binding,[11] or a change of redox state.[12] In addition, guest binding to, or release from, a helical host may be associated with single helix–double helix equilibrium,[13] with a light stimulus,[14] or with the ring contraction of a main-chain aromatic unit.[15]

Beyond isolated helices, one major challenge in foldamer science is the design of abiotic tertiary structures. Early attempts consisted of simply connecting several secondary folded modules with limited interactions between them.[16] Recent progress includes the consistent spatial arrangement of several abiotic helices,[17] as well as aromatic helix and sheet combinations.[18] The increasing size and sophistication of these structures provide opportunities for enhancing the amplitude and complexity of conformational responses to various stimuli. For instance, rotation about a single bond in a large folded object may give rise to a considerable and nontrivial change of molecular shape. Along this line, we now report the reversible, light-induced, switching between different conformations within a helix-sheet-helix aromatic amide foldamer. Specifically, we discovered a foldamer sequence that undergoes unexpected conformation dynamics leading to a noncanonical fold, and these dynamics can be reversibly controlled by means of an intramolecular photoreaction between two anthracene subunits.

The dimerization of anthracenes under irradiation by light is one of the most studied photochemical reactions. The reversible [4+4] cycloaddition of two anthracene molecules results in a photodimer connected by covalent bonds.[19] For substituted anthracenes, *syn*/*anti* and parallel/antiparallel (i.e., head-to-head and head-to-tail) isomeric products may form. Products with opposite dipole orientations are generally favored unless molecular or supramolecular constraints guide the reaction.[20,21] Thus, related 1,8-diazaanthracenes (i.e., pyrido-[3,2-g]quinolines) undergo quantitative antiparallel photodimerization in solution (Figure 1a; see Figure S1 in the Supporting Information).[22] Recently, we have shown that, when incorporated in aromatic oligoamide β-sheet foldamers, 1,8-diazaanthracene units formed parallel stacks

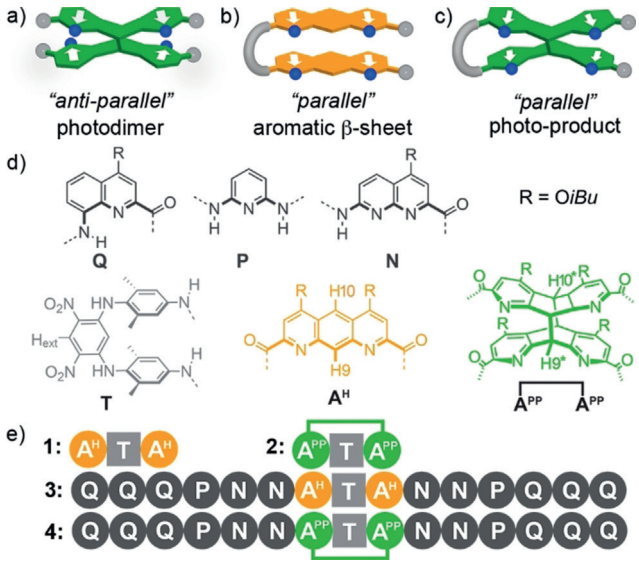

Figure 1. Cartoon representations of: a) an antiparallel diazaanthracene photodimer; b) a parallel arrangement of strands in a diazaanthracene β-sheet, and c) a parallel diazaanthracene photo-product in an aromatic β-sheet. In (a,b,c) white arrows indicate local dipole orientation and blue spheres indicate nitrogen atoms. d) Color coded formula and associated letters corresponding to amino acid, diamine, and diacid monomers. e) Oligoamide sequences **1**–**4**. Note that **2** and **4** are the photoproducts of **1** and **3**, respectively. The terminal A^H and Q units of these sequences have a methyl ester group and an 8-nitro group (instead of an 8-amino function), respectively.

favored by a better π-π overlap (Figure 1 b).[18] This observation led us to consider the production of parallel photoproducts guided by folding (Figure 1 c). The model compound **1** was prepared to test this hypothesis (see Scheme S1). It comprises two 1,8-diazaanthracenes,[23] A^H, separated by a dinitro-diamino-benzene turn,[24] T. Upon irradiation under anaerobic conditions at $320 < \lambda < 390$ nm using a 50 W lamp and appropriate cutoff filters, ^{1}H NMR monitoring showed the quantitative conversion of **1** into a single new product having the same mass in 20 minutes (see Figure S1). New signals of the former diazaanthracene H10 and H9 protons were found as singlets at $\delta = 5.35$ and 5.70 ppm (see Figure S1). These chemical shift values are consistent with a [4+4] photoreaction and the lack of H9*-H10* scalar coupling indicates that the parallel photoproduct **2** has formed (Figure 1 c; see Figures S1 and S2).[25] Such a quantitative parallel photoreaction guided by folding is remarkable. It reflects not only that the antiparallel aromatic β-sheet is disfavored, but also that its conformation is not conducive of a photoreaction (see Figure S16). As expected, the reaction was shown to be thermally reversible: in $C_2D_2Cl_4$, **2** was stable at 328 K but quantitatively converted back into **1** upon heating at 393 K for 15 hours (see Figures S3 and S4). In contrast, attempts to photochemically revert the reaction yielded by-products.

We then planned to test this photoreaction within a larger foldamer structure. The sequence **3** (Figure 1 e), comprising two conical Q_3PN_2 helical hexameric segments attached on both sides of a central A^HTA^H sheet was designed and synthesized (see Schemes S2 and S3). We have previously observed that a related sequence having a longer, three-stranded ATATA sheet folds in a canonical manner with its two helical segments stacked on each side of the central aromatic β-sheet.[18] With only two strands, as in **3**, a β-sheet is expected to mediate a helix handedness reversal leading to a plane symmetrical conformation noted (*M*,*P*)-*s***3** (see energy minimized models in Figure 2 e; see Figure S17). In line with earlier observations,[18] the ^{1}H NMR spectrum of **3** in [D_6]acetone shows one set of sharp lines whose multiplicity is

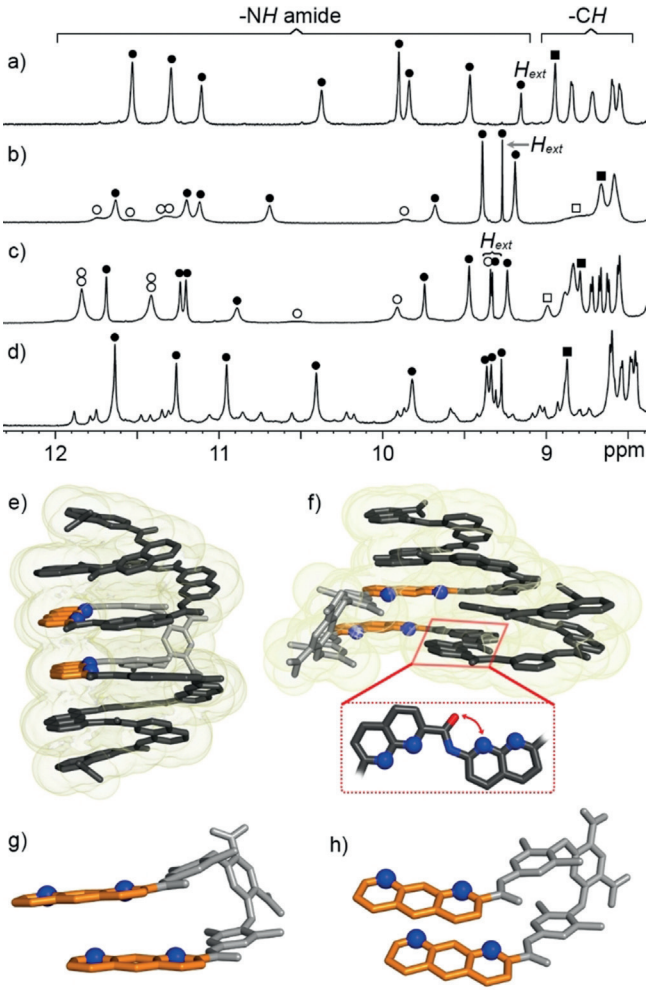

Figure 2. Part of the 700 MHz ^{1}H NMR spectra of **3** (1 mM) at: a) 298 K in [D_6]acetone; b) 298 K in $CDCl_3$; c) 233 K in $CDCl_3$, and d) 213 K in CD_2Cl_2. Signals assigned to symmetrical (*M*,*P*)-*s***3** and unsymmetrical (*M*,*P*)-*u***3** are marked with black (●) and empty (○) circles, respectively. The black and empty squares denote the amino protons of the turn unit for (*M*,*P*)-*s***3** and (*M*,*P*)-*u***3**; respectively. e) Side-view of the energy-minimized molecular model using Merck Molecular Force Field static (MMFFs) of plane symmetrical (*M*,*P*)-*s***3.** f) Front view of the structure in the solid state of unsymmetrical (*M*,*P*)-*u***3**. The zoom highlights the rotation of a helical segment about an amide-naphthyridine bond. A red double-headed arrow denotes a local electrostatic repulsion. g,h) Zoom on the diazaanthracene β-sheet turn unit in (*M*,*P*)-*s***3** (from e) and (*M*,*P*)-*u***3** (from f), respectively. The model and X-ray structures are shown in tube representation with color coded monomers as in Figure 1. Blue balls indicate endocyclic nitrogen atoms. Transparent yellow isosurfaces represent the volume of the foldamer. Hydrogen atoms, side chains and solvent molecules are not shown for clarity.

consistent with an overall symmetrical (*M,P*)-*s***3** structure (Figures 2a; see Figure S5). However, the ^{1}H NMR spectrum of **3** in $CDCl_3$ revealed a more complex situation. The symmetrical species that prevails in [D_6]acetone is also present but a second set of broad signals indicates coexistence with an other species in slow exchange on the NMR time scale (Figure 2b). Upon cooling in $CDCl_3$ down to 233 K, the proportion of this species increased to exceed 50% and signals remained somewhat broad (Figure 2c; see Figures S7 and S8). In CD_2Cl_2, the signals sharpened at 243 K and below (see Figure S10), and revealed a number of amide resonances compatible with a dissymmetrical structure (Figure 2d; see Figure S10).

Solid-state investigations shed light on the conformational behavior of **3**. X-ray quality single crystals were grown by slow diffusion of n-hexane into a chloroform solution.[26] The solid-state structure revealed an unanticipated unsymmetrical conformation in which a helical domain has undergone a large flip to stack underneath the other helix (Figure 2f), and to which the dissymmetrical species observed in solution may tentatively be assigned.[27] This conformer, which we named *u***3**, is accessible from (*M,P*)-*s***3** through a 180° rotation about a single aryl–amide bond between two N units. Apart from that, both helical segments and the parallel aromatic β-sheet fold as expected. The single-bond rotation results in a repulsive electrostatic interaction between an amide oxygen atom and an adjacent naphthyridine endocyclic nitrogen atom (Figure 2f). This repulsion is apparently compensated by favorable contacts including through the antiparallel stacking of the second quinoline of one helix and a naphthyridine of the other helix and through the filling of the cavity of one helix by an isobutoxy side chain of the other helix (see Figure S14). These contacts would not occur for β-sheets with three or more aromatic strands, hence the absence of unsymmetrical conformer for longer parent sequences.[18] Moreover, the unsymmetrical conformer *u***3** possesses a large flat aromatic surface, enabling stacking of two molecules in the solid state (see Figure S14). Conformer *u***3** in principle exists as a mixture of two degenerate (*M,P*) and (*P,M*) states. The mechanism of their interconversion is unclear, in particular, whether or not it must transit through *s***3** (equilibria 1 and 2 in Figure 3).

In both the crystal structure of *u***3** and the energy minimized model of *s***3**, the two A^H units have a parallel orientation but are significantly offset (ca. 2.4 Å, Figures 2g,h) and not ideally preorganized for a [4+4] cycloaddition. Photoirradiation of **3** in $CDCl_3$ was nonetheless performed. Thus, a 1 mM solution was irradiated under an argon atmosphere and a photoreaction took place, albeit at a slower rate than with **1**. As followed by ^{1}H NMR spectroscopy, 80% of the starting oligomer **3** was converted into its photoproduct **4** after 1 hour of irradiation (Figure 4b). Complete conversion was reached within 4 hours (Figures 4c,e). The slower kinetics may be assigned to the not-ideal conformation mentioned above and to favorable interactions within *u***3** and *s***3** that must be disrupted for the reaction to take place. The parallel arrangement of the photoproduct was again ascertained by the emergence of two singlets at $\delta = 4.8$ and 5.5 ppm assigned to H10* and H9*, respectively. In addition, the ^{1}H NMR spectrum of **4** shows a single set of signals and indicates a symmetrical structure.

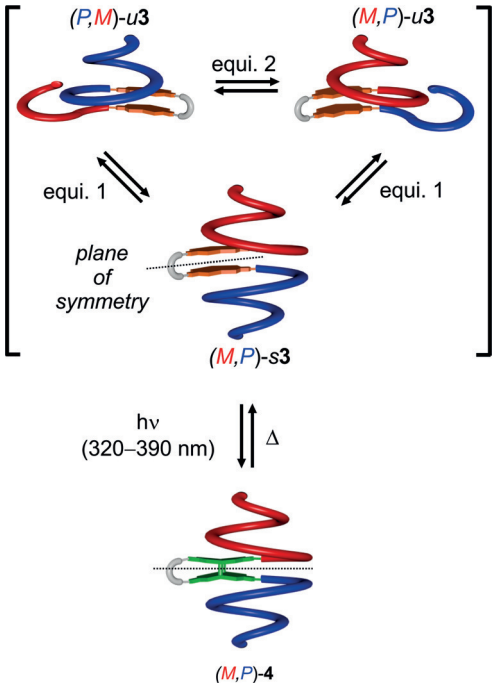

Figure 3. Schematic representation of the equilibria and reactions involved in the switching process. Equilibria 1 and 2 do not require helix handedness inversion. Yet the ensemble of *u***3** and *s***3** species is in slow equilibrium with another mirror-imaged (thus degenerate) ensemble obtained through handedness reversal of both helical segments. The thermally reversible photoreaction of the two parallel A^H units locks the conformation in a plane symmetrical state. *P* and *M* helices are shown as blue and red tubes, respectively. The diazaanthracene β-sheet and its photoproduct are color coded in orange/grey and green/grey, respectively.

The symmetrical conformation with *P* and *M* helices, and the parallel arrangement of the photoproduct were confirmed by a solid-state structure of **4**.[26] Crystals grew upon slowly diffusing methanol into a chloroform solution. The structure was solved in the *P*−1 space group and revealed that the helices remain above and below the butterfly-shaped photoreacted β-sheet in a canonical structure even though proper stacking onto the A^H units is no longer possible. Thus, the photoreacted turn is fully embedded in-between the two helices, with H9* protons pointing towards the concave side of the sheet whereas H10* protons point towards to convex side of the sheet (Figures 4f–h). If compared to the symmetrical conformer prior to photoirradiation, the overall foldamer length increased from 2.05 to 2.15 nm as a result of photoadduct formation and also possess an enlarged cavity.

Starting from the equilibrating mixture of *u***3** and *s***3** conformers, light thus allows one to lock the molecule in a plane-symmetrical conformation that has been expanded by the photoreaction, and thus to remove unsymmetrical conformers (Figure 3), as when longer sheets are present. The reaction between the two A^H units is selective: cross-reaction with other heterocycles in the structure is avoided.[28] Furthermore, the photoproduct can be thermally reverted to the mixture of *u***3** and *s***3**. Heating **4** in $CDCl_3$ at 328 K led to

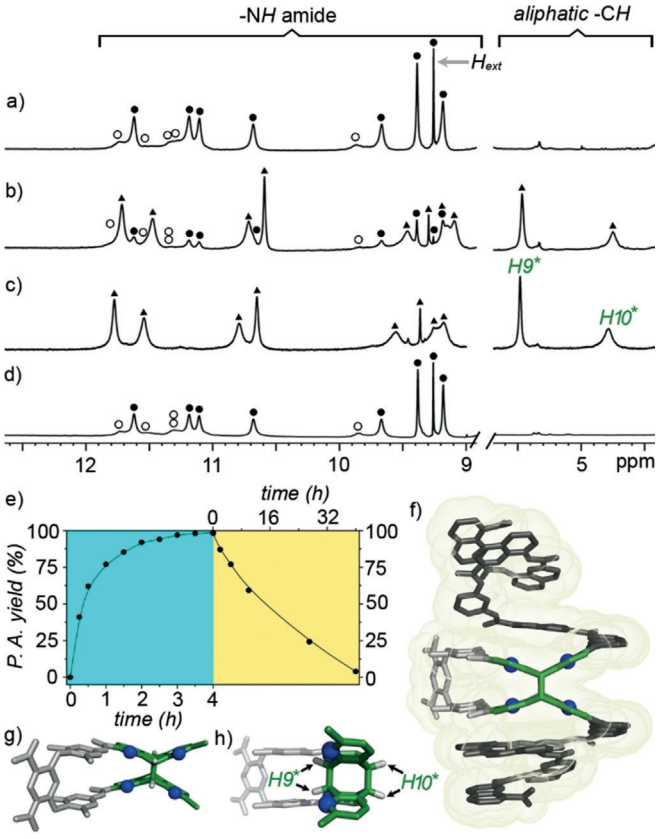

Figure 4. Part of the 700 MHz ^{1}H NMR spectra of at 298 K of **3** (1 mM in $CDCl_3$) under photoirradiation after a) 0 min; b) 60 min.; and c) 4 h. d) Evolution after incubating sample (c) at 328 K for 40 h. Signals of *s***3** and *u***3** are denoted with black (●) and white (○) circles, respectively. Black triangles indicate signals of the photoproduct **4**. e) Kinetic monitoring (^{1}H NMR) of: (left) the photoreaction of **3** yielding **4** and (right) the thermolysis of **4** back into **3**. f) Crystal structure of **4**. g,h) Front and side-view of the photoreacted β-sheet highlighting the parallel arrangement. The structure is shown in tube representation and the monomers are color coded as in Figure 1. Blue balls denote endocyclic nitrogen atoms. Side chains, solvent molecules, and hydrogen atoms are not shown for clarity.

about 50% of conversion after 16 hours. Quantitative recovery of **3** required almost two days. One should note that, despite being slow, this reverse reaction is perfectly clean and anyway much faster than for the photoproduct **2**, which is stable at this temperature. The lower stability of **4** possibly reflects a higher strain imposed by folding.

In summary, we have discovered an unanticipated unsymmetrical conformer in helix-sheet-helix foldamers, and found that the quantitative parallel photoreaction of diazaanthracenes within aromatic β-sheets exclusively and reversibly produces symmetrical conformers. The cleanness of the photoreaction suggests that it could be implemented multiple times within a given aromatic foldamer sequence, thus leading to a global stiffening and length extension of the molecule, or that it could be reliably used to control guest binding and release. Efforts toward these objectives are currently in progress and will be reported in due course.

Acknowledgements

This work was supported by the post-doc program of the Excellence Initiative of Bordeaux University (B.G.). This work has benefited from the facilities and expertise of the Biophysical and Structural Chemistry platform (BPCS) at IECB, CNRS UMS3033, Inserm US001, and Bordeaux University.

Conflict of interest

The authors declare no conflict of interest.

Keywords: foldamers · molecular switches · oligomers · photochemistry · X-ray crystallography

How to cite: *Angew. Chem. Int. Ed.* **2019**, *58*, 8063–8067
Angew. Chem. **2019**, *131*, 8147–8151

[1] M. F. Perutz, *Nature* **1972**, *237*, 495–499.
[2] B. T. DeVree, J. P. Mahoney, G. A. Velez-Ruiz, G. F. Rasmussen Soren, A. J. Kuszak, E. Edwald, J.-J. Fung, A. Manglik, M. Masureel, Y. Du, R. A. Matt, E. Pardon, J. Steyaert, B. K. Kobilka, R. K. Sunahara, *Nature* **2016**, *535*, 182–186.
[3] K. Svoboda, C. F. Schmidt, B. J. Schnapp, S. M. Block, *Nature* **1993**, *365*, 721–727.
[4] T. Sakamoto, M. R. Webb, E. Forgacs, H. D. White, J. R. Sellers, *Nature* **2008**, *455*, 128–132.
[5] G. Guichard, I. Huc, *Chem. Commun.* **2011**, *47*, 5933–5941.
[6] For reviews and books see: a) *Molecular Switches*, 2nd ed. (Eds.: B. L. Feringa, W. R. Browne), Wiley-VCH, Weinheim, **2011**; b) *New Frontiers in Photochromism* (Eds.: M. Irie, Y. Yokoyama, T. Seki), Springer, Japan, **2013**; c) T. van Leeuwen, A. S. Lubbe, P. Štacko, S. J. Wezenberg, B. L. Feringa, *Nat. Rev. Chem.* **2017**, *1*, 0096.
[7] a) D. Roke, C. Stuckhardt, W. Danowski, S. J. Wezenberg, B. L. Feringa, *Angew. Chem. Int. Ed.* **2018**, *57*, 10515–10519; *Angew. Chem.* **2018**, *130*, 10675–10679; b) R. Mogaki, K. Okuro, T. Aida, *J. Am. Chem. Soc.* **2017**, *139*, 10072–10078; c) J. Gurke, S. Budzak, B. M. Schmidt, D. Jacquemin, S. Hecht, *Angew. Chem. Int. Ed.* **2018**, *57*, 4797–4801; *Angew. Chem.* **2018**, *130*, 4888–4893; d) S. Fredrich, R. Gostl, M. Herder, L. Grubert, S. Hecht, *Angew. Chem. Int. Ed.* **2016**, *55*, 1208–1212; *Angew. Chem.* **2016**, *128*, 1226–1230; e) I. Aprahamian, *Chem. Commun.* **2017**, *53*, 6674–6684; f) H. Qian, S. Pramanik, I. Aprahamian, *J. Am. Chem. Soc.* **2017**, *139*, 9140–9143; g) K. M. Chan, D. K. Kolmel, S. Wang, E. T. Kool, *Angew. Chem. Int. Ed.* **2017**, *56*, 6497–6501; *Angew. Chem.* **2017**, *129*, 6597–6601; h) J. R. Hemmer, S. O. Poelma, N. Treat, Z. A. Page, N. D. Dolinski, Y. J. Diaz, W. Tomlinson, K. D. Clark, J. P. Hooper, C. Hawker, J. Read de Alaniz, *J. Am. Chem. Soc.* **2016**, *138*, 13960–13966; i) D. Zhao, T. van Leeuwen, J. Cheng, B. L. Feringa, *Nat. Chem.* **2017**, *9*, 250–256.
[8] T. Miyagawa, A. Furuko, K. Maeda, K. Katagiri, Y. Furusho, E. Yashima, *J. Am. Chem. Soc.* **2005**, *127*, 5018–5019.
[9] a) D. Mazzier, M. Crisma, M. De Poli, G. Marafon, C. Peggion, J. Clayden, A. Moretto, *J. Am. Chem. Soc.* **2016**, *138*, 8007–8018; b) F. G. A. Lister, B. A. F. Le Bailly, S. J. Webb, J. Clayden, *Nat. Chem.* **2017**, *9*, 420–425.
[10] a) C. Tie, J. C. Gallucci, J. R. Parquette, *J. Am. Chem. Soc.* **2006**, *128*, 1162–1171; b) Z. Yu, S. Hecht, *Angew. Chem. Int. Ed.* **2011**, *50*, 1640–1643; *Angew. Chem.* **2011**, *123*, 1678–1681.

[11] N. Ousaka, K. Shimizu, Y. Suzuki, T. Iwata, M. Itakura, D. Taura, H. Iida, Y. Furusho, T. Mori, E. Yashima, *J. Am. Chem. Soc.* **2018**, *140*, 17027 – 17039.
[12] E. Ohta, H. Sato, S. Ando, A. Kosaka, T. Fukushima, D. Hashizume, M. Yamasaki, K. Hasegawa, A. Muraoka, H. Ushiyama, K. Yamashita, T. Aida, *Nat. Chem.* **2011**, *3*, 68 – 73.
[13] a) F. C. Parks, Y. Liu, S. Debnath, S. R. Stutsman, K. Raghavachari, A. H. Flood, *J. Am. Chem. Soc.* **2018**, *140*, 17711 – 17723; b) Y. Hua, Y. Liu, C.-H. Chen, A. H. Flood, *J. Am. Chem. Soc.* **2013**, *135*, 14401 – 14412.
[14] Y. Hua, A. H. Flood, *J. Am. Chem. Soc.* **2010**, *132*, 12838 – 12840.
[15] G. Lautrette, C. Aube, Y. Ferrand, M. Pipelier, V. Blot, C. Thobie, B. Kauffmann, D. Dubreuil, I. Huc, *Chem. Eur. J.* **2014**, *20*, 1547 – 1553.
[16] a) N. Delsuc, M. Hutin, V. E. Campbell, B. Kauffmann, J. R. Nitschke, I. Huc, *Chem. Eur. J.* **2008**, *14*, 7140 – 7143; b) N. Delsuc, S. Massip, J.-M. Léger, B. Kauffmann, I. Huc, *J. Am. Chem. Soc.* **2011**, *133*, 3165 – 3172; c) W. Ichinose, J. Ito, M. Yamaguchi, *Angew. Chem. Int. Ed.* **2013**, *52*, 5290 – 5294; *Angew. Chem.* **2013**, *125*, 5398 – 5402; d) C. Tsiamantas, X. de Hatten, C. Douat, B. Kauffmann, V. Maurizot, H. Ihara, M. Takafuji, N. Metzler-Nolte, I. Huc, *Angew. Chem. Int. Ed.* **2016**, *55*, 6848 – 6852; *Angew. Chem.* **2016**, *128*, 6962 – 6966; e) H.-Y. Hu, J.-F. Xiang, Y. Yang, C.-F. Chen, *Org. Lett.* **2008**, *10*, 69 – 72.
[17] S. De, B. Chi, T. Granier, T. Qi, V. Maurizot, I. Huc, *Nat. Chem.* **2018**, *10*, 51 – 57.
[18] A. Lamouroux, L. Sebaoun, B. Wicher, B. Kauffmann, Y. Ferrand, V. Maurizot, I. Huc, *J. Am. Chem. Soc.* **2017**, *139*, 14668 – 14675.
[19] H. D. Becker, *Chem. Rev.* **1993**, *93*, 145 – 172.
[20] For reviews see: a) H. Bouas-Laurent, A. Castellan, J.-P. Desvergne, R. Lapouyade, *Chem. Soc. Rev.* **2000**, *29*, 43 – 55; b) H. Bouas-Laurent, A. Castellan, J.-P. Desvergne, R. Lapouyade, *Chem. Soc. Rev.* **2001**, *30*, 248 – 263.
[21] a) J. Tanabe, D. Taura, N. Ousaka, E. Yashima, *J. Am. Chem. Soc.* **2017**, *139*, 7388 – 7398; b) P. Kissel, D. J. Murray, W. J. Wulftange, V. J. Catalano, B. T. King, *Nat. Chem.* **2014**, *6*, 774 – 778; c) Y. Kawanami, S. Y. Katsumata, M. Nishijima, G. Fukuhara, K. Asano, T. Suzuki, C. Yang, A. Nakamura, T. Mori, Y. Inoue, *J. Am. Chem. Soc.* **2016**, *138*, 12187 – 12201; d) M. J. Kory, M. Worle, T. Weber, P. Payamyar, S. W. van de Poll, J. Dshemuchadse, N. Trapp, A. D. Schluter, *Nat. Chem.* **2014**, *6*, 779 – 784; e) A. Nakamura, Y. Inoue, *J. Am. Chem. Soc.* **2003**, *125*, 966 – 972; f) J. Yao, Z. Yan, J. Ji, W. Wu, C. Yang, M. Nishijima, G. Fukuhara, T. Mori, Y. Inoue, *J. Am. Chem. Soc.* **2014**, *136*, 6916 – 6919; g) A. V. Lunchev, S. A. Morris, R. Ganguly, A. C. Grimsdale, *Chem. Eur. J.* **2019**, *25*, 1819 – 1823.
[22] a) H. Ihmels, C. J. Mohrschladt, A. Schmitt, M. Bressanini, D. Leusser, D. Stalke, *Eur. J. Org. Chem.* **2002**, 2624 – 2632; b) D. Jouvenot, E. C. Glazer, Y. Tor, *Org. Lett.* **2006**, *8*, 1987 – 1990; c) E. Berni, C. Dolain, B. Kauffmann, J.-M. Léger, C. Zhan, I. Huc, *J. Org. Chem.* **2008**, *73*, 2687 – 2694; d) M. Li, A. D. Schluter, J. Sakamoto, *J. Am. Chem. Soc.* **2012**, *134*, 11721 – 11725; e) P. Payamyar, M. Servalli, T. Hungerland, A. P. Schutz, Z. Zheng, A. Borgschulte, A. D. Schluter, *Macromol. Rapid Commun.* **2015**, *36*, 151 – 158.
[23] M. L. Singleton, N. Castellucci, S. Massip, B. Kauffmann, Y. Ferrand, I. Huc, *J. Org. Chem.* **2014**, *79*, 2115 – 2122.
[24] a) L. Sebaoun, V. Maurizot, T. Granier, B. Kauffmann, I. Huc, *J. Am. Chem. Soc.* **2014**, *136*, 2168 – 2174; b) L. Sebaoun, B. Kauffmann, T. Delclos, V. Maurizot, I. Huc, *Org. Lett.* **2014**, *16*, 2326 – 2329.
[25] Note: in the antiparallel photoproduct, these protons would appear as two doublets as the result of *J3* scalar coupling (see Figure S1). A detailed investigation of the photoreaction will be published elsewhere.
[26] CCDC 1897516 (**3**) and 1897517 (**4**) contain the supplementary crystallographic data for this paper. These data can be obtained free of charge from The Cambridge Crystallographic Data Centre.
[27] The NMR spectrum of freshly dissolved crystal shows that equilibrium is reached too fast to be monitored by this technique.
[28] H. Masu, I. Mizutani, T. Kato, I. Azumaya, K. Yamaguchi, K. Kishikawa, S. Kohmoto, *J. Org. Chem.* **2006**, *71*, 8037 – 8044.

Manuscript received: February 22, 2019
Accepted manuscript online: April 8, 2019
Version of record online: May 12, 2019

